CHAPTER THREE

D.C. ELECTRICAL RESISTIVITY, CURIE TEMPERATURE, THERMOELECTRIC POWER OF $Zn_xMg_{1-x}Fe_2O_4$ FERRITE SYSTEM DOPED WITH 0.01 MOL. WT. % ZrO_2

CHAPTER - III

3.1 Introduction :

The mechanism of charge transport can be understood from the study of electrical conductivity, thermoelectric power, Hall coefficient and magnetoresistance. The electrical and magnetic properties exhibited by ferrites are the direct consequences of charge transport mechanism, which is highly influenced by physico-thermal history and chmical composition. The theoretical analysis of the said phenomena can be had from variation of the density and mobility of charge carriers with temperature.

Ferrite have a wide range of resistivity variation from 10^{-3} ohm cm to 10^{+9} ohm.cm. Due to wide range of resistivity variation they are preferred at high frequency applications, rather than metals and alloys. The study of D.C electrical resistivity with temperature furnishes an useful information regarding application point of view, and also it throws some light on conduction mechanism. The low resistivity of Magnetite (Fe_3O_4) is due to the presence of Fe^{2+} and Fe^{3+} ions situated on the crystallographically equivalent sites (1).

Oxides containing a substantial concentration of metal ions in different valance states on crystallographically equivalent sites requires small activation energy reflecting in low resistivity. The resistivity of a given oxide system generally decreases with mixed valancy concentration. The iron rich ferrites (2) shows low resistivity of the order of 10^{-2} ohm cm and similar is the case of Lanthanum magnetite (3). The change of semiconducting to pseudo-metallic in these cases occurs near magnetic transformation temperature.

The breaks and discontinuties in log (ρ) versus 1/T plots for many ferrites have been observed by Komer et al.[4] and the same were also observed by Verway et al.[1] in case of Mn-Ni ferrite. Van Uitret et al.[5] have reported the effect of surface grinding on the resistivity of Ni-Zn ferrite. The observed reduction of resistivity in this case, is attributed by him to voltalization of zinc during heat treatment, encouraging the formatioin of Fe^{2+} ions on the surface.

The conduction in ferrites is due to exchange of electrons from Fe^{2+} to Fe^{3+} ions situated on a same, equivalent lattice site that is octahedral site by hopping mechanism. Recently Klinger[6] has reviewed the conduction mechanism, pointing out that, the hopping of polaron is the main process of conduction in ferrites. He has also suggested two phase mechanism for hopping of polarons.

Resistivity of ferrites markedly influenced by cation distribution, crystal structure, porosity, grain size, impurity inclusions, chemical or oxidation states and the varied scattering mechanisms. Ferrites by nature are semiconductors, when impurity is added to it, becomes extrinsic semiconductor. In almost all semi-conductors conduction at higher temperature is due to holes and electrons, which are thermally excited. The predominant charge carriers in the conduction process at any instant of temperature, can be understood by the sign of Seebeck coefficient (α) and the Hall coefficient. Basic information of the conductioin process below Curie temperature can be derived from the study of Hall coefficient. The considerable insight in the conduction process can be had from thermo-electric power measurements, which is relatively easy for ferrites having resistivity less than 10^8 ohm-cm.

High resistivity and low loss factor make ferrites an industrially important materials. They give noiseless operation at high frequency, hence used in high frequency inductances and memory devices. High resistivity of ferrites and garnets at room temperature can be employed into transmission lines, cavities and wave guide.

This chapter deals with the study of resistivity variation with composition and temperature. Also the efforts are made to measure the thermoelectric power with temperature. The Curie temperatures are measured experimentally by suing the experimental set-up described in the section 3.3b. The results and discussion are given at the end section of this chapter and lastly the references.

3.2 Conduction in Ferrites :

Basic investigation regarding the mechanism of charge transport was done by Verway et al.[1]. The simultaneous presence of ferrous and ferric ions on crystallographically equivalent sites, usually the octahedral sites gives low conductivity. The extra electron on a ferrous ion requires a little energy to move to a similarly situated adjacent ferric ion. The valance states of the two ions gets interchanged. Under the influence of an electric field, the extra electrons are being considered to establish the conduction current, jumping or hopping from one iron ion to the another.

Ferrites being the semiconductors by nature, their resistivity (ρ) decreases with increase in temperature in accordance with the relation

$$\rho = \rho_0 \exp. (\Delta E/K_T) \qquad \ldots \quad (3.1)$$

where ΔE is the activation energy required to cause the electron jump from one iron ion to the other. T be the absolute temperature and K the Boltzman constant, ρ_o is the temperature independent term, that only depends on the nature of material. The conductivity of high resistivity oxides can be increased by the addition of small amounts of foreign oxides to the structure, whose metal ions have valancies different from the host cations. The substitution of a cation of low valance state gives rise p type conductivity, whereas substitution of a cation of high valance state gives rise to n type conductivity.

Apart from inherent properties of materials, the conductivity will also be influenced by the following factors.

1) Polycrystalline ferrites are characterised by pores, if these are filled with air or other different material influence the conductivity.

2) The grain size of the individual crystallites in polycrystalline sample can affect the grain to grain contacts and thus influence the conductivity paths which in turn changes the resistivity.

3) Chemical inhomogenity caused during preparation also influences the conduction, and is mainly governed by heat treatment.

Klinger[6] has reviewed the conduction mechanism in ferrites, who has suggested two phase mechanism for hopping process, of polarons.

3.2.1 D.C. electrical resistivity

The variation of bulk resistivity (ρ) with temperature 'T' in ferrites is given by the relation (3.1). The breaks and discontinuities that occurs in resistivity versus 1/T plots, which shows change in activation energy (ΔE). By using this change in activation energy, the resistivity variation with temperature can

be studied in different regions. In general almost all ferrites exhibit two regions of conductivity variation i.e. a single break in resistivity versus temperature, which occurs at Curie tempeature Tc.

But in some cases, three distinct regions of conductivity variation are also reported by Nanba et al.[7] in case of copper ferrite, Ghani et al.[8] for Cu-Ni system, Joshi et al.[9] for Mg-Zn ferrite and Todkar et al.[10] for copper ferrite. In three region conductivity plots there are two breaks in the conductivity plots. First break in this case is denoted by Todkar et al.[10] as characteristic temperature 'Th'. It is seen that with increase of temperature of the sample decreases linearly the log resistivity, up to characteristic temperature 'Th'.

The IInd region in conductivity plot is attributed by Ghani et. al.[8] to the phase transition while by Nanba[7] to cation migration. Rezlescu[11] to cation ordering and Todkar et al.[10] to some new type of spin alignment. The second break in all these cases occurs at Curie temperature 'Tc'. The change of activation energy takes place while passing from ferri to para region. In general it is observed that the 'ΔE' values in para region are greater than ferri region, which is attributed to different mode of conduction that occurs above Tc. In ferrites conduction in this region is due to thermally activated hopping process.

3.2.2 Electron hopping and polarons :

The most common effect of the electron phonon interaction is seen in the temperature dependance of the electrical resistivity. A more subtle effect of the electron phonon interaction is the apparent increase of electron mass in metals and insulators, because the electrons drags the heavy ion are

along with it. In an insulator the combination of the electron and its strain field is known as a polaron[12]. The electrostatic interaction between a conduction electron or hole and near by ions may result in a displacement of the ions and hence in polarisation of the surrounding region, so that charge carrier becomes situated at the centre of polarisation potential well. If this well is deep enough, a carrier may be trapped at a lattice site, and its transition to a neighbouring site may be determined by thermal activation. This process has been considered as the 'hopping mechanism'.

The electron take part in diffusion process by jumps, which takes place from one site to the other. The process of thermal activation is encountered in ionic diffusion and ionic conductivity. Heikes and Johnston[13] has derived an expression for the mobility of charge carriers during the hopping mechanism given by the relation

$$\mu = \frac{e^2 a^2 wo}{KT} \exp. \left(\frac{-q}{KT}\right) \quad \ldots \quad (3.2)$$

where 'a' is the distance between nearestneighbours wo - frequency of vibration and 'q' be the activation energy for hopping process.

The expression (3.2) has been used by many authors in the discussion of electrical conductivity. With the advent of polaron theory it has become evident that expression (3.2) represents a special case of much more complicated relationship between mobility 'μ' and a lattice parameter of ionic lattice. The conductivity σ can be written in terms of the concentration of charge carriers and their mobility 'μ' is given by

$$\sigma = e (n_e \mu_e + n_h \mu_h) \quad \ldots \quad 93.3)$$

This relation is also used by many authors to explain the conduction in ferrites

To calculate the mobility 'u', one requires a knowledge of spatial extent of a polarisation potential well. If the polarisation potential well extends over many lattice units in the crystal, then excess of charge be considered to interact with dielectric continum.

This type of model has been employed by Forhlich[15] to formulate inter action Hamiltonion for large polarons. He has introduced the parameter known as electron-phonon coupling constant for the discussion of polarons. It is common to speak about large and small polarons. The actual polaron size can be inferred from free energy consideration. Formation of small polaron is favoured when coupling constant is large and conduction band is narow. At sufficiently low temperature a small polaron behaves as a particle moving in a narrow band. At high temperature small polaron absorbs one or more phonon and moves from site to site by hopping mechanism.

The strength of electron lattice interaction is measured by the dimensions less coupling constant 'α' given by

$$\frac{1}{2}\alpha = \frac{\text{deformation energy}}{\hbar\, WL} \qquad \ldots \qquad (3.3)$$

where WL - Longitudinal optical phenon frequency near zero wave vector, and 1/2 α the number of polarons which surrounds a slow moving electron in crystal lattice. The effective mass of the polaron is given by

$$M^*_{pol} = \left(\frac{1-0.00\alpha^2}{1-1/6\alpha+0.034\alpha^2} \right) \qquad \ldots \qquad (3.4)$$

where M^* is the effective band mass of electron in the undeformed lattice. If $\alpha << 1$ then expression (3.4) can be approximated as

$$M^*_{pol} \cong M^* \left(1+\frac{1}{6}\alpha\right) \qquad \ldots \qquad (3.5)$$

(α), the coupling constant, which is always positive.

It can be seen that the mobility in transition metal oxides is strongly temperature dependent. The conductivity linked with the polaron will be a dominant transport mechanism. There is strong experimental evidence for the existance of small polarons and the hopping process.[17]

3.2.3 Experimental technique for data collection
(* D.C. electrical resistivity)

The resistivity measurements were made on two probe conductivity cell specially designed and fabricated in the departmental work-shop. The block-diagram of two probe conductivity cell is as shown in figure 3.1, and the necessary circuit diagram as shown in figure 3.2.

The conductivity cell consists of two cylindrical brass electrodes fitted in the porcelain discs. A material sample is sandwitched between the electrodes with the help of connecting rods, provided with nuts. The electrically insulated copper wire was used for external connections. Silver foil for good electrical contact was placed on the pellet specimen. The entire assembly was then kept in the temperature regulated furnace. The furnace temperature was then slowly increased. The calibrated chromel-alumel thermocouple was used for the temperature measurement. Digital multimeters were used for precise measurement of current and voltages. The d.c. electrical resistivity measurement for slow cooled samples of $Zn_xMg_{1-x}Fe_2O_4$ ferrite, system doped weith 0.01 mol wt.% ZrO_2 were carried out in the temperature range of 30°C to 500°C.

The resistivity (ρ) was calculated by uising the relation

$$\rho = \frac{\pi r^2}{t} \cdot \frac{V}{I} \qquad \ldots \quad 3.6)$$

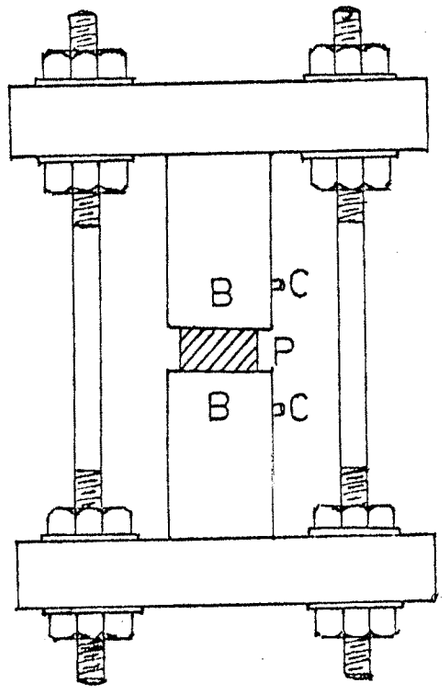

P - Pellet

B - Brass electrode

C - Connection lead

Block diagram of pellet holder

Fig. 3.1

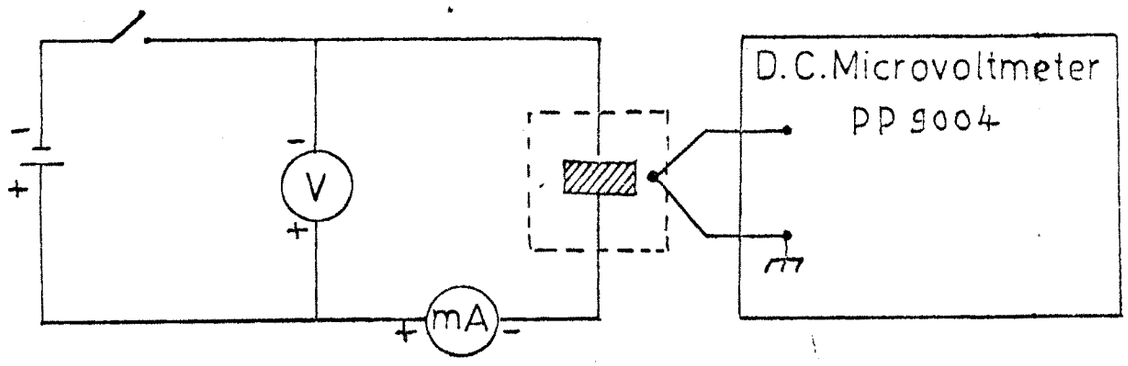

A schematic circuit diagram for d.c.conductivity measurements

Fig. 3.2

The graph of log (ρ) versus 1/T for each sample was plotted and from the plots, Curie temperatures were recorded. (see fig. 3.5 to 3.10). The values of ΔE, and Curie temperatures from log (ρ) versus 1/T plots are presented in table 3.1.

3.3 Curie Temperature :

The critical temperature for a ferromagnetic or ferrimagnetic material at which magnetic transformation takes place is called Curie temperature. It is the temperature below which, there is a spontaneous magnetisation, in the absence of an externally applied magnetic field and above wehich the material is paramagnetic. In the disordered state above Curie temperature thermal energy overrides any interactions between the local magnetic moment. Below Curie temperature these interactions are predominant, and cause the local moments to order or to allign, in such a way that there is a net spontaneous magnetisation.

In ferrimagnetic materials the course of magnetisation with temperature may be more complicated, but the spontaneous magnetisation disappears at the Curie temperature. Curie temperature can be determined from the magnetisation versus temperature plots or from the related anamolies. For the present investigation, we have used resistivity versus temperature plots for the determination of Curie temperature. The plots of Log (ρ) versus1/T show breaks and discontinuities at Curie temperature 'Tc' which can be ascribed to several sources. Komer and Klivshin[15] have observed changes in the activation energies, for conduction at high temperature in several ferrites, and co-related it with the ferrimagnetic Curie temperature. This offers strong evidence for

the influence of magnetic ordering on conductivity of ferrites.[14] The breaks may also be due to some change in dominant conduction mechanism.

Many physical properties shows change in behaviour at the Curie tempe rature. There is a peak in specific heat and in magnetic permiability at Curie temperature. There is a change in elastic properties and thermal expansivity. The Curie temperature can be altered by changes in composition, pressure and other thermodynamic parameters.

3.3.1 Experimental set-up for 'Tc' measurement

Loria et al.[15] have suggested a method for determination of Curie temperature, which suffers from a drawback, that along with the pellet, the core of electromagneti gets heated. This may damage the enamel of the elect-romagnet wire, which may lead to short circuit. At the same time it requires more current to obtain substantial magnetisation. Hence we have modified the same method, and used to determine the Curie temperature of the system $Zn_xMg_{1-x}Fe_2O_4$ ferrites doped with 0.01 mol. wt.% ZrO_2

In this modified technique the core is not subjected to temperature to the temperature of furnace and it involves induction technique for the magnetisation of the pellet sample. The sectional cut view of this method is as shown in figure (3.3). The temperature of the furnace at which pellet falls is accurately measured by calibrated chromel alumel thermocouple. The values of experimental Curie temperature are given in table number 3.1.

3.4 Thermoelectric Power :

When two dissimilar metal wires are joined together to form the junction and if the junctions are maintained at different temperatures an

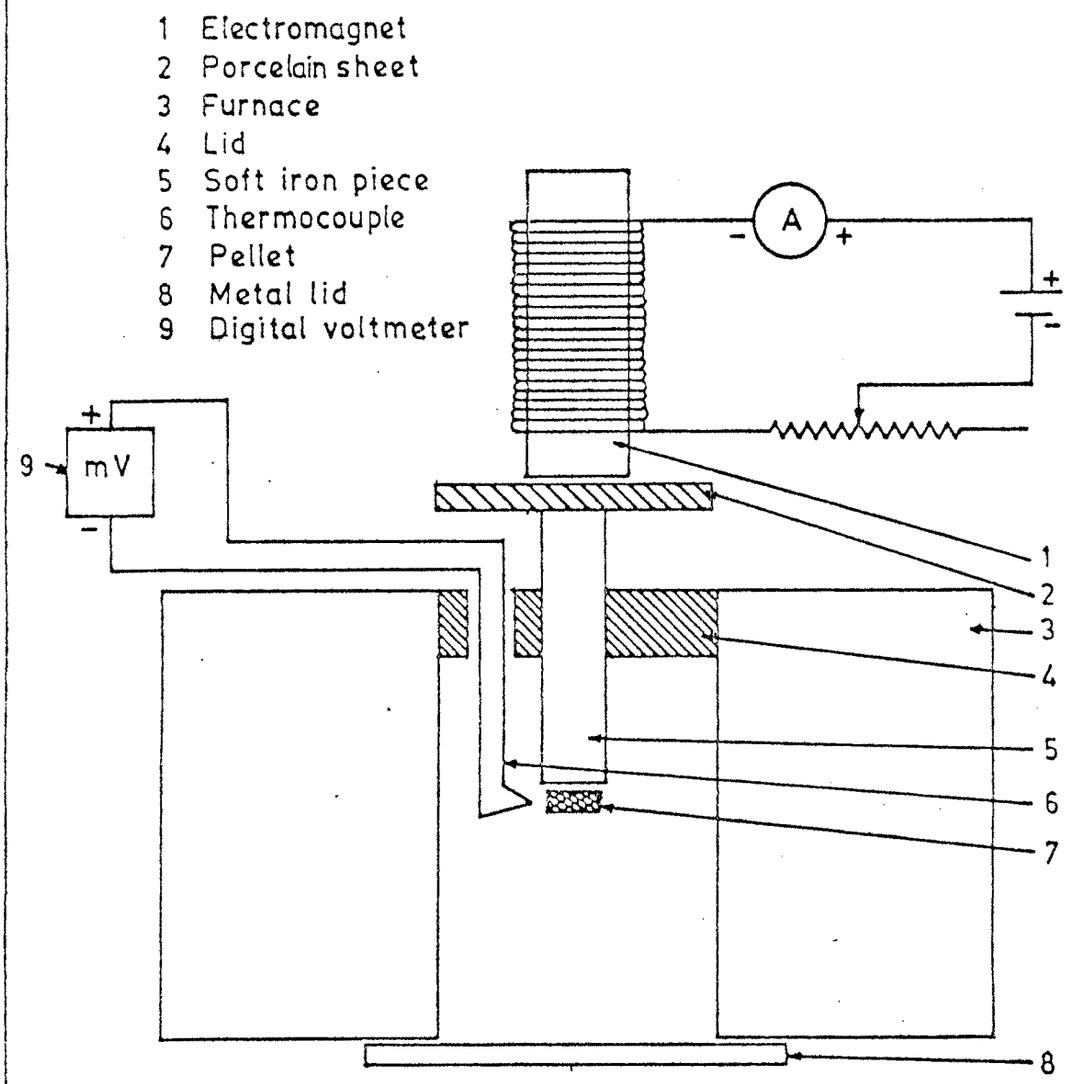

Fig.3-3 : SET UP FOR DETERMINATION OF CURIE TEMPERATURE(Tc).

electron-motive force is developed. This effect was observed by Seebeck and hence called seebeck effect. The Seebeck coefficient is denoted by 'α', which is the ratio of change of electromotive force across the two junctions, to the temperature difference between the junctions.

The Seebeek effect is a sort of diffusion process in which holes and electrons at hot end with higher kinetic energy as compared to cold end and hence constitutes the current. The Seebeek coefficient 'α' for semiconductors with both type of charge carriers is given by

$$\alpha = (\alpha_n \sigma_n + \alpha_p \sigma_p) / (\sigma_n + \sigma_p) \quad \ldots \quad (3.7)$$

where

$$\sigma_n = n_e u_n \; ; \; \sigma_P = P_e u_p$$

$$\alpha_n = \frac{-K}{e} [\, A_n - E_F/KT \,]$$

$$\alpha_p = \frac{K}{e} [\, A_p + E_g + E_F/kT \,]$$

where n and p are electrons and hole densities, 'u_n' and 'u_p' are the electron and hole mobilities respectively. 'E_F' is the Fermi energy and 'E_g' is the band gap.

For a partially filled band, the Seebeek coefficient 'α' varies linearly with the temperature given by

$$\alpha_n = -(\pi^2 K^2/3e) T \, [\, d \ln \sigma(E)/d_T \,]_{E=E_F} \quad \ldots \quad (3.8)$$

where $\sigma(E)$ is the conductivity, which Fermi level is at 'E'. The term $[\, d \ln \sigma(E)/d_T \,]$ can be approximated accordingly whether the Fermi energy is temperature dependent or not. The temperature dependance of thermo-electric power for a ferrite having only one type of charge carriers is given by[16]

$$\alpha = \frac{K}{e}\left[\text{in} \left(\frac{No}{n} - 1 \right) + \frac{q}{KT} \right] \quad \ldots \quad (3.9)$$

where K = Boltzman constant

e = electronic charge

No = Concentration of trivalent ions on the octahedral sites.

n = Concentration of Fe^{2+} ions.

The term 'q' is the part of activation energy transported by the electrons, and T is the absolute temperature. The value of term 'a' is zero for Mn ferrites[17] and 1 eV for other cases.[18] The temperature dependence of Seebeck coefficient enables to determine the sign ofcharge carriers and density variation of charge carriers.

3.4.1 Experimental set up

(Seebeck coefficient measurement)

For the measurement of Seebeck coefficient (α), the specimens were taken in the form of pellets. The specimen was held in sample holder made from brass block as shown in figure (3.4). There are two methods for the measurement of Seebeck coefficient 'α', the integral and differential, out of these two, for present study later was used. In differential technique a temperature difference is established between the two ends by heating one end with the auxillary heater. Heater consist of spiral coil of nicrome wire (30 ohm per cm) of 20 to 30 ohm resistance. This coil was inserted in a cylindrical electrode. A dimerstat (15 amperes and 220 v) was used to control the temperature.

The whole assembly was kept in temperature regulated furnace. Due care was taken to avoid the sudden heat changes due to air flow. The temperature of both the junctions were accurately measured by embeded cromel

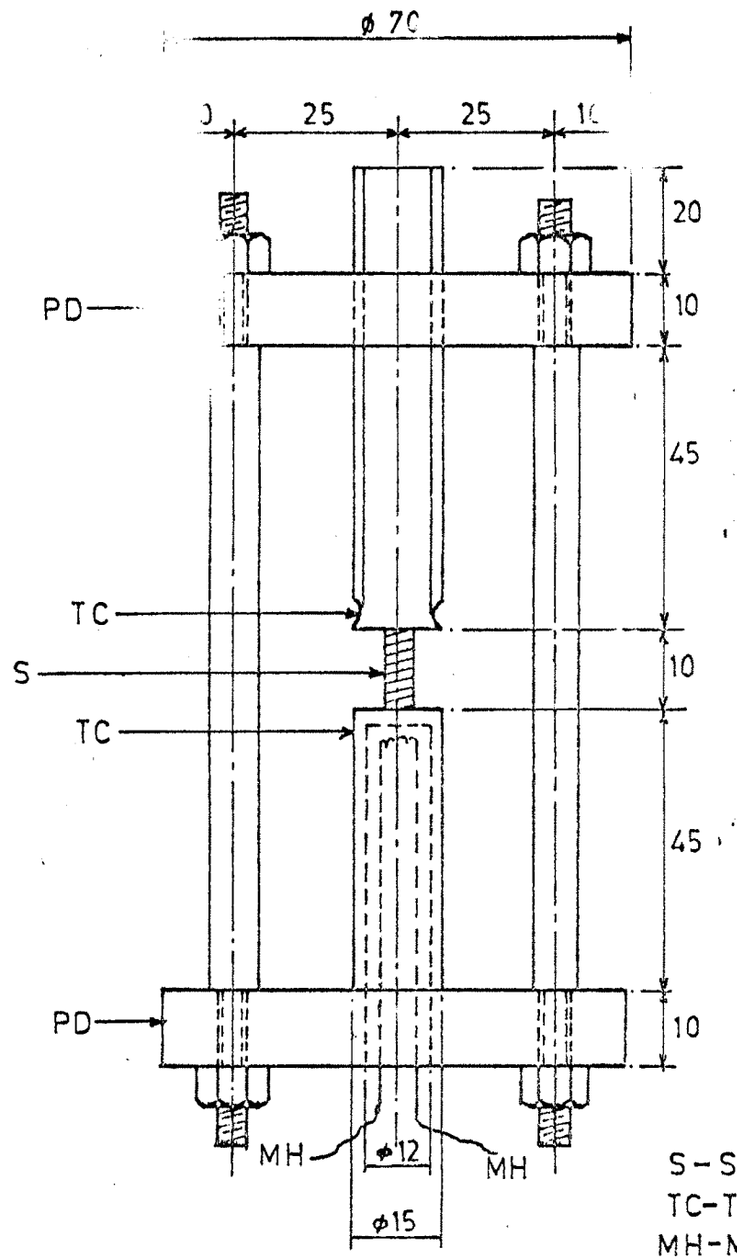

SAMPLE HOLDER FOR MEASURING THERMO E.M.F.

Fig. 3·4

alumel thermocouple. Temperature was measured on a digital multimeter and a sign of electromotive force was carefully noted.

Seebeck coefficient at different furnace temperature was calculated by taking the ratio of voltage across the pellet specimen, to the temperature difference maintained across the parallel faces of the specimen. The measurement for slow cooled samples of $Zn_xMg_{1-x}Fe_2O_4$ ferrite system doped with 0.01 mol. wt % zirconium oxide, were made in the temperature range of 6°C to 500°C. The graph of temperature versus Seebeck coefficient 'α' and plotted and are presented in figures 3.11 to 3.16.

3.5 Results and Discussion :

The variation of log (ρ) versus 1/T has been studied for the ferrite system $Zn_xMg_{1-x}Fe_2O_4$ (where x=0, 0.2, 0.4, 0.6, 0.8, 1.0), doped with 0.01 mol. wt.% ZrO_2, in the temperature range from 300°K to 800°K. These plots are presented in figures 3.5 to 3.10. The variation in the resistivity exhibit peculiar trends. The samples L0, L2, L4, L6, (x=0, 0.2, 0.4, 0.6) show three distinct regions of conductivity variation, while sample L8 (for x=0.8) shows two regions of conductivity variation. The sample L10 (x=1) show a single region of conductivity, having no breaks and discontinuity in conductivity variation, that is no transition at and above room temperature.

For L0, L2, L4, L6 samples the first break is denoted by characteristic temperature. 'Th', which is indicated on resistivity plots by a downward arrow. This nomenclature is adopted from literature[7,10]. The second break in these plots denotes the Curie temperature 'Tc' and is shown by upward arrow on these plots. For L8 sample there is only one break, and is denoted by the

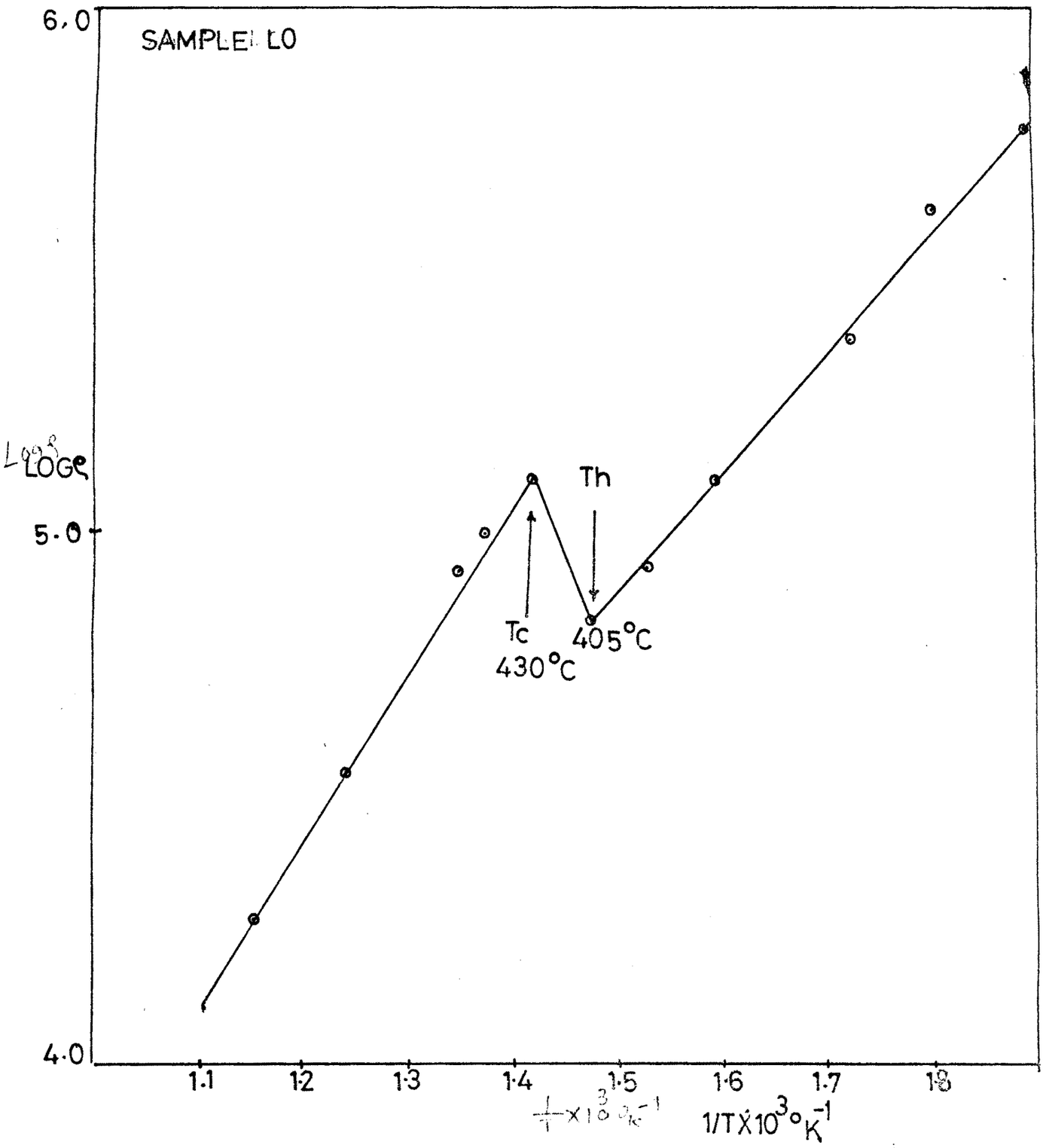

FIG : 3.5 - LOG e Vs 1/T X 10^3 $°K^{-1}$

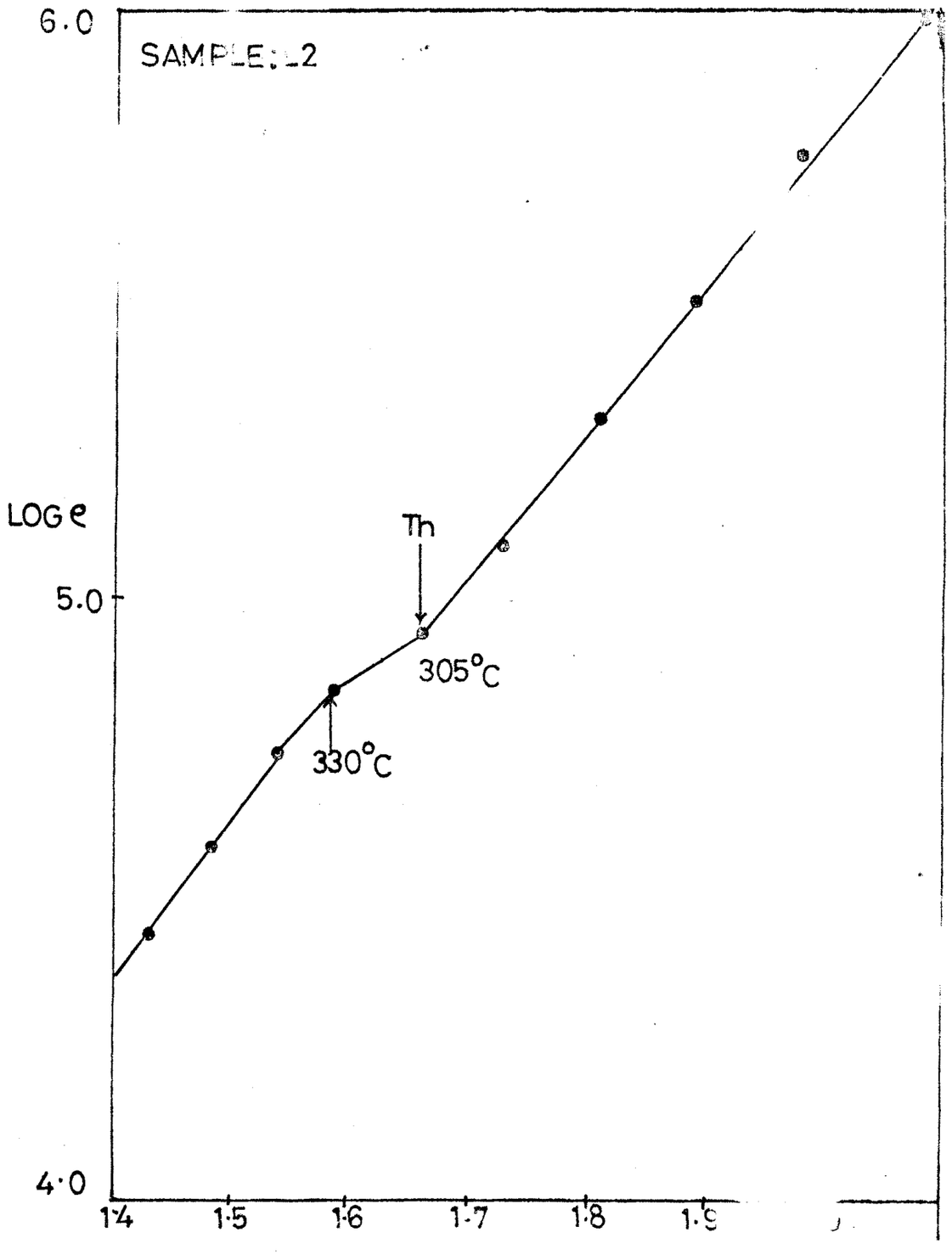

FIG: 3·6 – LOG ρ ✻ 1/T X 10^{3} °K^{-1}

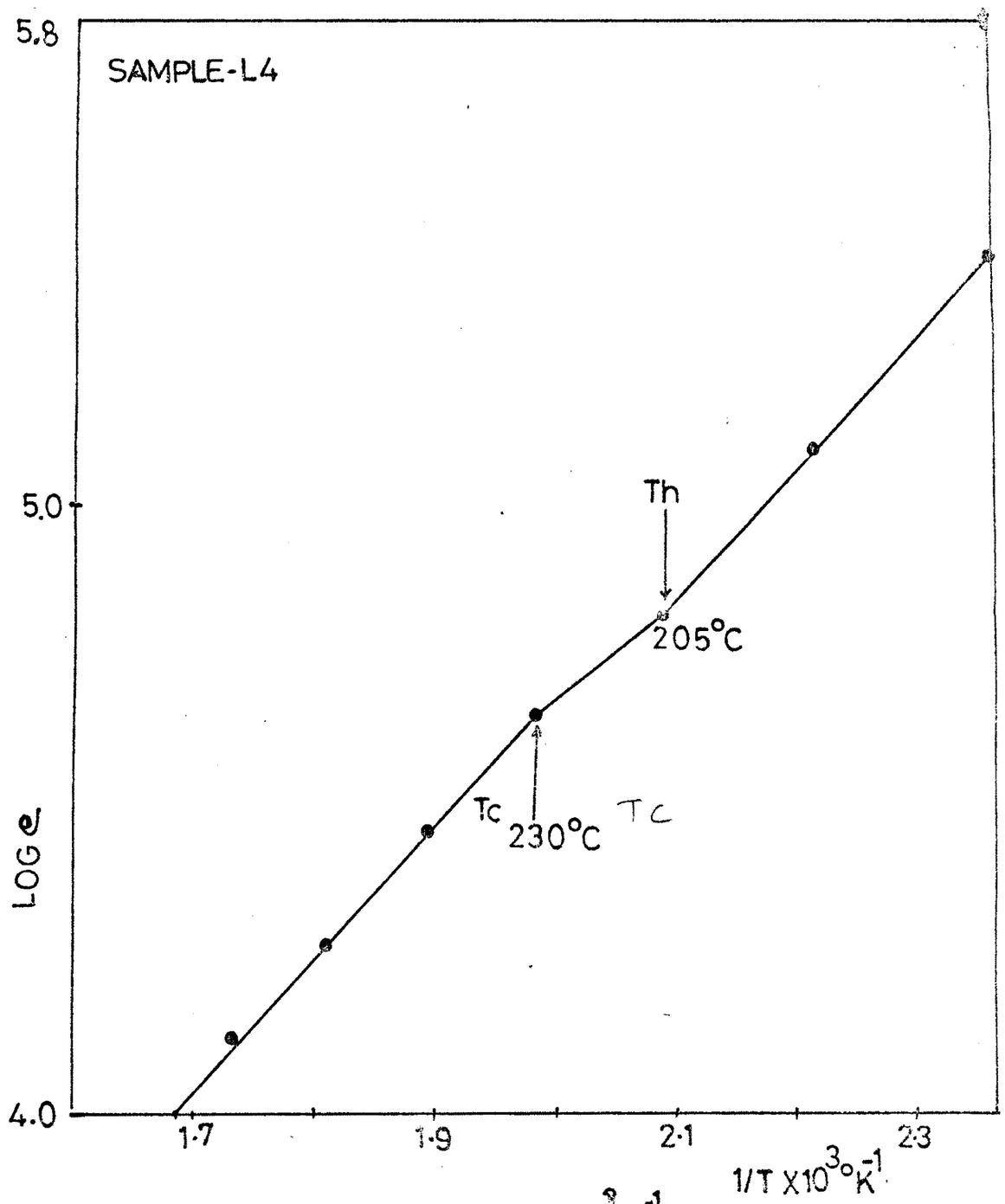

FIG: 3.7- LOG ρ Vs 1/T X 10^3 °K^{-1}

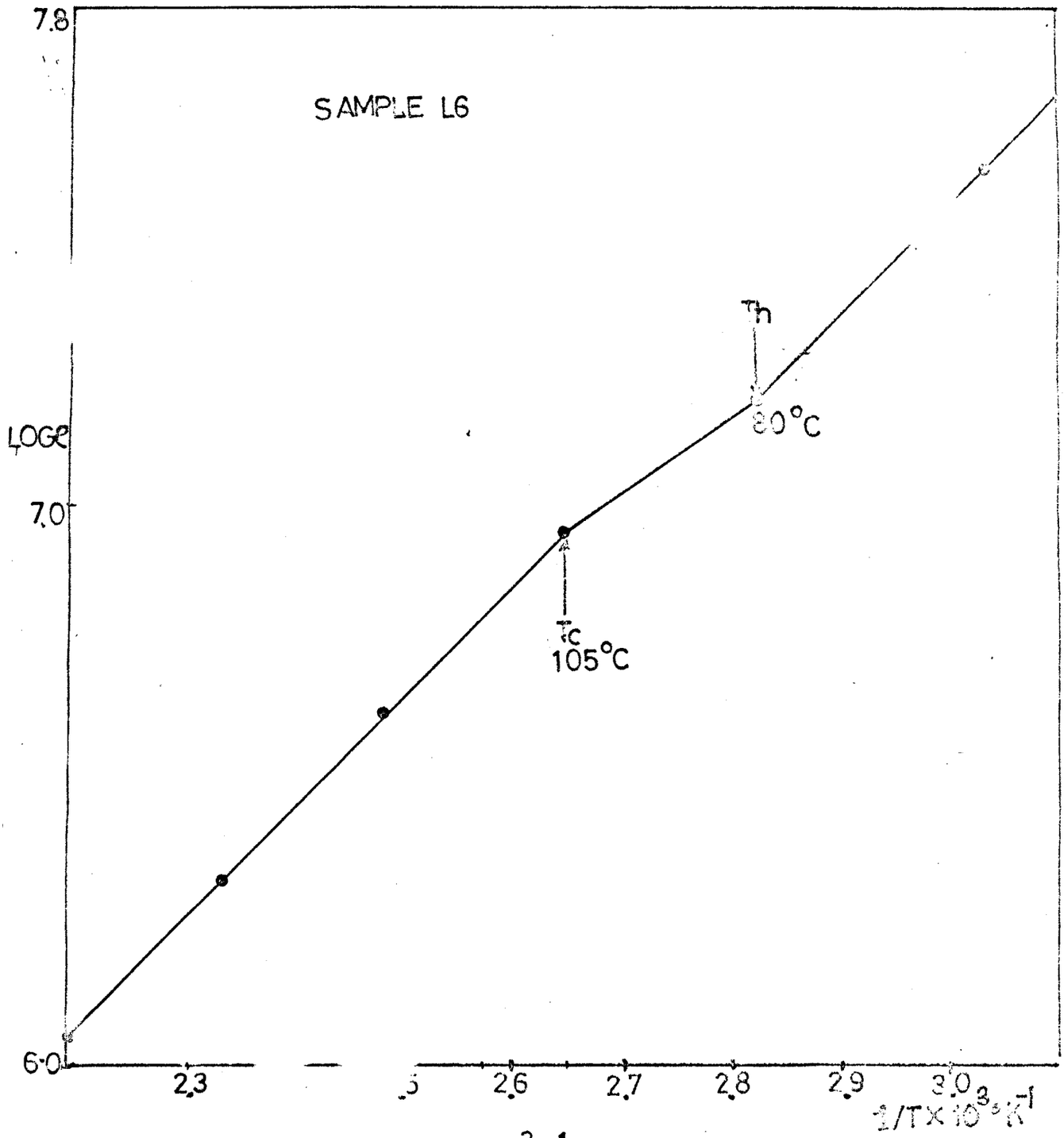

FIG:- 3.L . . LOGe X 1/T X 10^3 °K^{-1}

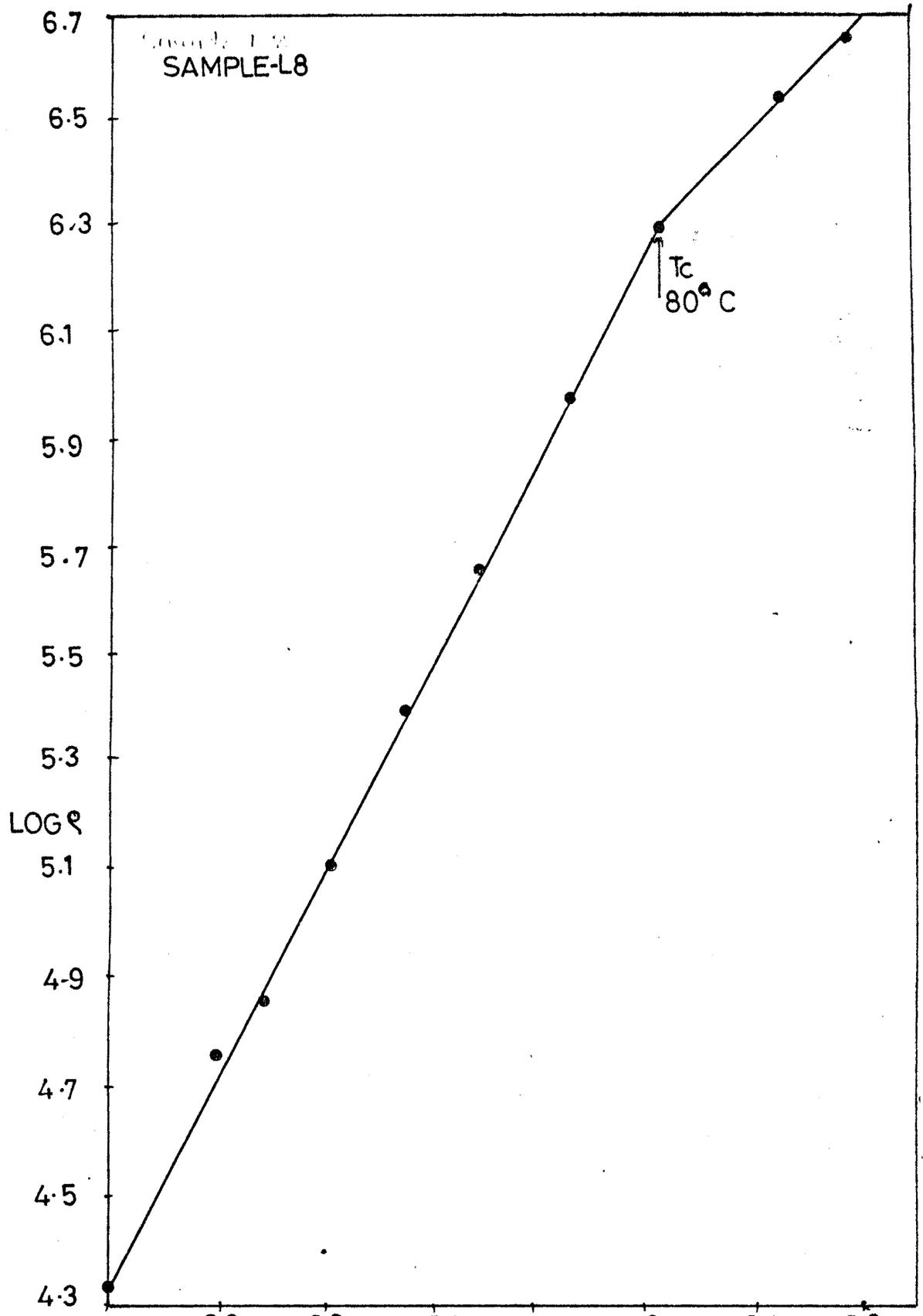

FIG: 3.9 :- LOG ρ Vs 1/T X 10^{3} K^{-1}

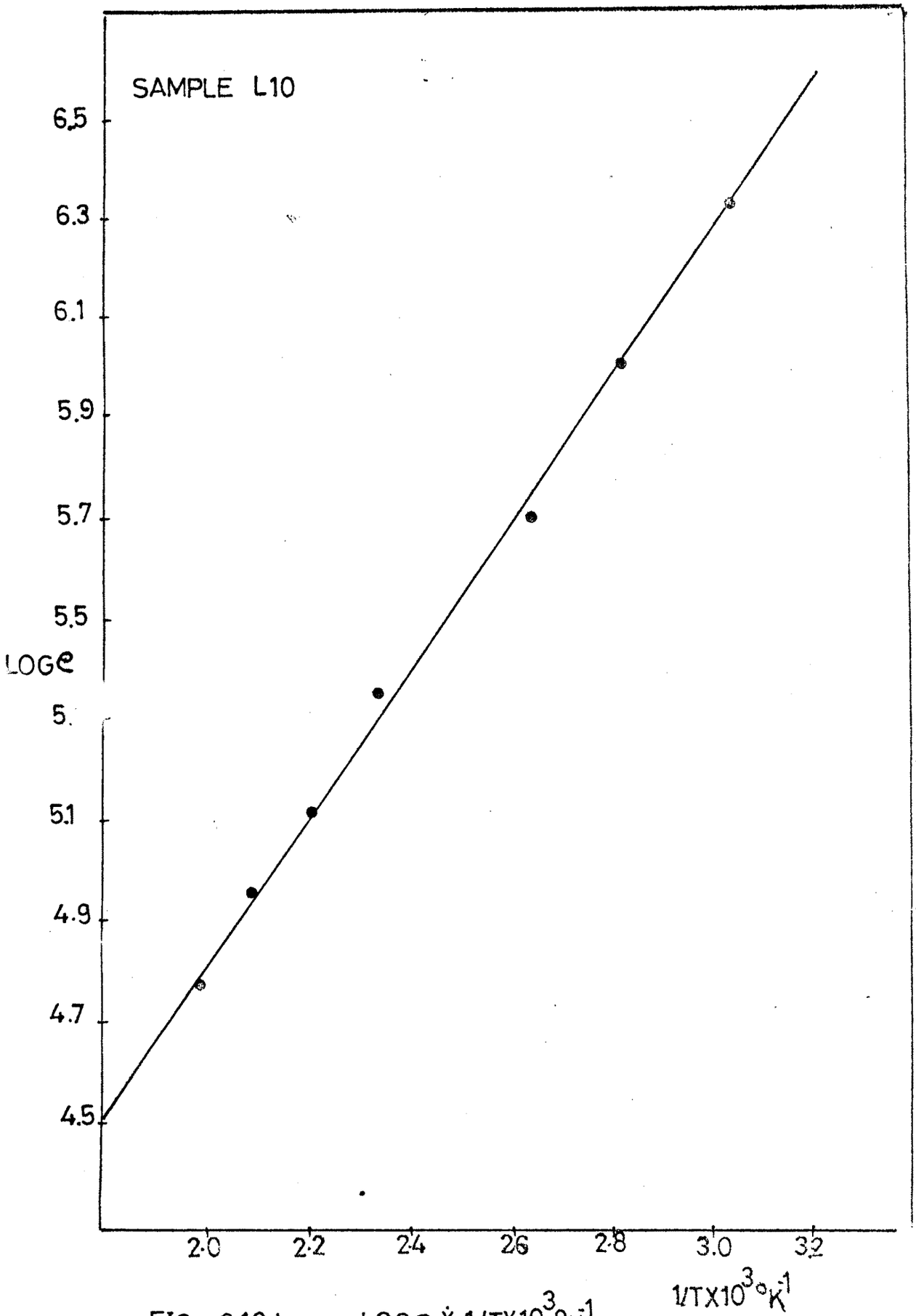

FIG- 3·10 : LOGe·Ẋ·1/TX10^3°K^{-1}

upward arrow, which corresponds to the Curie temperature 'Tc', and it does not exhibit the characteristic temperature 'Th'. The sample L10 shows no break in conductivity variation, and hence it is paramagnetic at and above room temperature. The value of 'Th', 'Tc' and ΔE for all these samples under investigation are presented in table 3.1.

Curie temperature 'Tc' for all the samples under investigation are measured by using experimental set up described in section 3.3(b). The measured 'Tc' values are presented in table 3.1, for comparison. Sample L10 does not show Curie temperature at and above room temperature.

The temperature dependance of Seebeck coefficient 'α' for the above samples in the temperature range 279°K to 800°K was also studied and the nature of variation is presented in figures 3.11 to 3.16.

Discussion :

The plots of log (ρ) versus 1/T show linear relation, which is characteristic of semiconducting materials. The temperature dependance of resistivity ' ' can be written as

$$\rho = \rho_0 \exp. \frac{\Delta E}{KT}$$

where ρ_0 is essentially a temperature independent term that depends on nature of the material. 'ΔE' is the activation energy and 'K' and 'T' have their usual meanings. The conductivity 'σ' can be expressed in terms of mobility μ and carrier densities by the relation

$$\sigma = e (n_e u_e + n_p u_p)$$

where n_e and n_p are the concentrations of electrons and holes respectively μ_n and μ_p are their mobilities respectively, and 'e' be the electronic charge

The electrical resistivity, the change in activation energy at Curie temperature, the change of activation energy with composition, and effect of impurity doping on activation energy can be explained in the light of hopping mechanism of polarons[11]. In ferrites conduction can be due to hopping of electrons from Fe^{2+} to Fe^{3+} ions on the octahedral sites. The energy required for this hopping process is known as the activation energy (ΔE). For electron hopping the value of E, is of the order of 0.2 eV or less [19]. On the other hand the polaron hopping requires higher order of ΔE.

The values of ΔE from table 3.1 indicate that in para region the hopping process of polaron is obviously favoured, in case of our ferrite system under investigation. Therefore, the theory of hoping of polarons due to thermal activation[6] can explain the observed conductivity variation. The temperature dependance of electrical conductivity in hopping process involves less temperature dependent carrier concentration but the mobility. The hopping mechanism itself involvs occasional excitation by lattice vibration of the carriers with high degree of probability. The mobility μ in hopping process is given by Heikes and Johnston[13] and is given by

$$\mu = \frac{ed^3\nu}{KT} \exp^{(-q/KT)}$$

Thus mobility of charge carriers is the central part deciding the activation energy, which depends on phonon spectrum of the crystal and local variation due to local surroundings on each other. Klinger's[6] two phase polaron model, throws some light on the low temperature conductivity as owing to thermally activated motion of polaron, while at high temperature conduction is via weakly activated hopping motion, or by tunneling.

Table 3.1

D.C. electrical resistivity of $Zn_xMg_{1-x}Fe_2O_4$ ferrite system doped with 0.01 mol. wt. % ZrO_2

Composition + 0.01 mol. wt. % ZrO_2	Sample Notation	ΔE		Characteristic temp. (Th)°C	Curie temp. from graph Tc °C	Curie temp. Exptl. Tc°C
		Para eV	Ferri eV			
$MgFe_2O_4$	L0	0.26	0.18	405	430	440.2
$Zn_{0.2}Mg_{0.8}Fe_2O_4$	L2	0.24	0.21	330	355	328.6
$Zn_{0.4}Mg_{0.6}Fe_2O_4$	L4	0.18	0.17	2.05	230	228.6
$Zn_{0.6}Mg_{0.4}Fe_2O_4$	L6	0.19	0.17	80	105	127
$Zn_{0.8}Mg_{0.2}Fe_2O_4$	L8	0.17	0.086	-	80	-
$ZnFe_2O_4$	L10	0.12	-	-	-	-

From table 3.1 it can be seen that values of activation energy (ΔE) in para region are greater than that of ferri region. It is also seen from table 3.1 that activation energy in Ferri region generally decreases with increase of Zn content. Similarly activation energy in para region follows the same trend to that of Ferri region. This can be attributed to the effect of the magnetic disordering in the conduction process, while changing from Ferri to para region[20]. The decrease of ΔE in both the regions with Zn content may be attributed to n type zinc ferrite, which substitutes the p type $MgFe_2O_4$ giving electrons in the lattice of $Zn_xMg_{1-x}Fe_2O_4$ ferrite, which requires less energy of activation for the hopping process. The Seebeck coefficient variation with temperature fig. (3.11) shows that sample L0 is n type above 380° K while all remaining samples above room temperature are n type.

The observation of three distinct regions in the conductivity variation of the system under investigation is in consistasnce with earlier reports in case of Zn-Ni[9] system, copper ferrite[7], Cu-Ni[8] system, and copper ferrite[10]. It can be observed that with increase in temperature of the sample decreases linearly the log resistivity upto characteristic temperature (Th) indicated by downward arrow in resistivity plots. The sort of change in slope of the resistivity plots indicates a transition from one region to the other. The samples L0, L2, L4, L6 are paramagnetic above 'Tc'. The differentiation between the three regions was done by Ghani et al.[28] in the light of change in activation energy (ΔE) and the behaviour of Seebeck coefficient (α).

The first region in resistivity plots of slow cooled $MgFe_2O_4$ ferrite doped with 0.01 mol. wt.% ZrO_2 (i.e. Lo) can be studied with the variation of 'α' in the temperature range 279° to 753° K (Fig. 3.11). The positive sign of α below 380°K indicate that the predominant charge carriers are holes, while

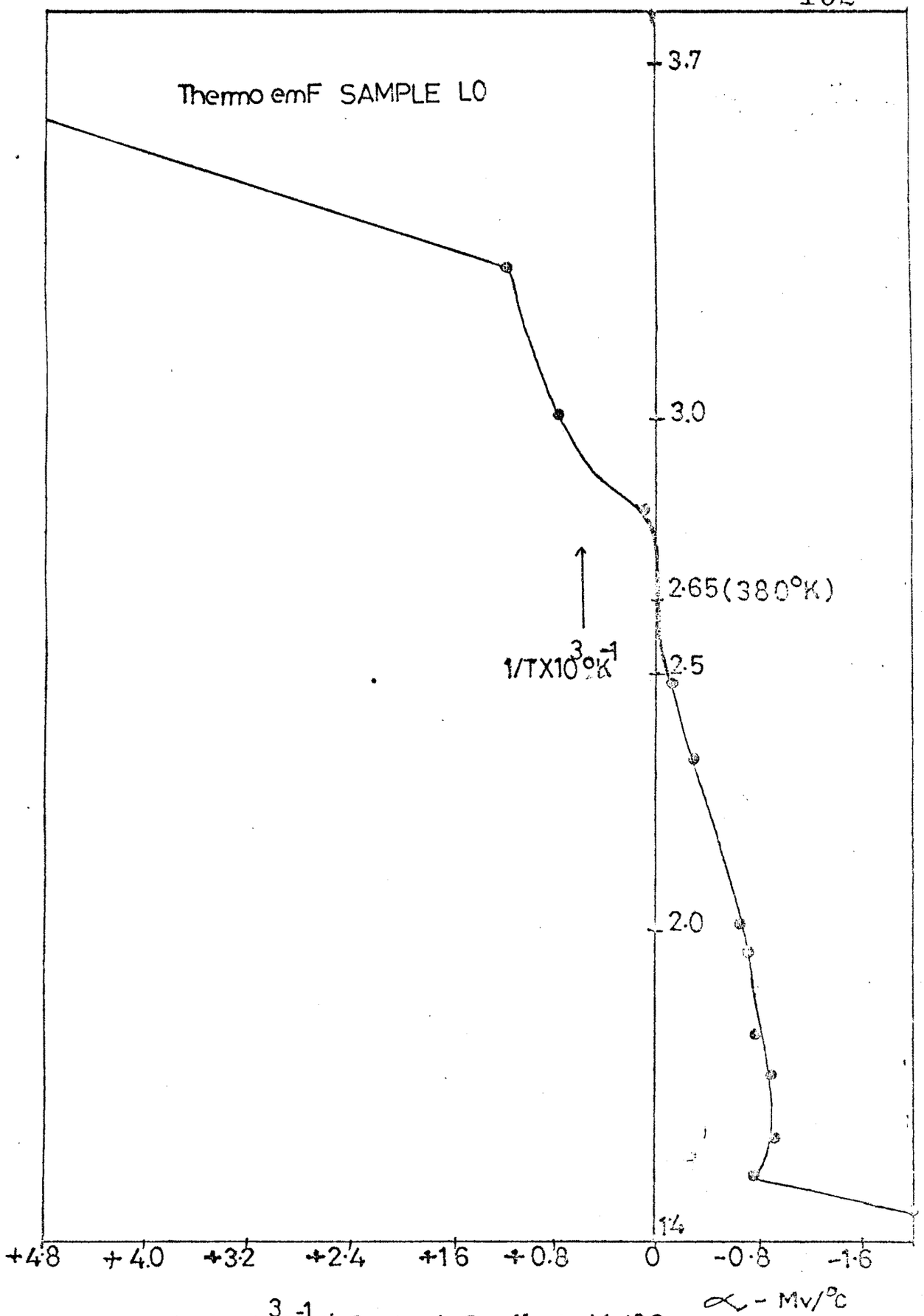

FIG - 3.11 : $1/T \times 10^{3}\,^{\circ}K^{-1}$ Vs Seebeck Coeff $\propto$ - Mv/°C

for higher than 380° K the majority carriers are electrons. This can be attributed to the fact that sample L0 is partly compensated in the first region by the presence of donor as well as acceptor centers, in the lattice of ferrites. The formation of both types of centres are expected from the loss of oxygen during the sintering process, and role of impurity that added.

The loss of oxygen may cause a part of cations to occupy interstitial sites, which acts as acceptors and the p type carriers may be identified[22] as hole on oxygen O^{2-} ion. The added impurity can help in charge compensation that reduces some of Fe^{3+} ions to Fe^{2+} ions, which acts as donor centres. It is well known that Magnesium ferrite is p type[23], at and above room temperature. Above 380° K in L0, above 302° K in L2, and for all remaining samples above room temperature predominant charge carriers are electrons. The observed values of activation energy clearly show increase of conductivity, with addition of 0.01 mol. wt. % ZrO_2. The dissolution of ZrO_2 in the spinel lattice leads to the creation of divalent iron ions and vacancies. Similar argument is putforth in case of Ni-Zn ferrites doped with 0.2 mol. wt.% V_2O_5 by Ram Narayana et al.[24] and TiO_2 doped Mn-Zn ferrites by Johnson et al.[25]

The addition of ZrO_2 within the solubility limit may increase Fe^{2+} ions concentration. However the oxidation reduction equilibrium for iron requires that in the absence of any other charge an increase in cation vacancy accompanies an increase in the Fe^{2+} to Fe^{3+} ratio. Johnston et al.[27] also have reached the similar conclusion in case of Mn-Zn ferrites doped with Ti^{4+}, by estimating quantitatively the vacancy and Fe^{2+} ion concentration, with increase of Ti^{4+} ions. The same conclusions are also due to Ram Narayan

et al.[24] in case of Ni-Zn ferrite doped with V_2O_5. The quantitative analysis of Fe^{2+} ion formation is proposed by Johnston et al.[27] and we have also proposed the same in case of our ferrite system doped with 0.01 mol. wt.% ZrO_2 in case of Zn-Mg ferrites, because both are tetravalent. Thus addition of every Zr^{4+} ion reduces 7/3 Fe^{3+} ions into 7/3 Fe^{2+} ions forming a pairs of Fe^{2+} triplet analogus to Ti^{4+} in Mn-Zn ferrites.[27] Thus addition of single Zr^{4+} ion in the lattice forms two Fe^{2+} ions, and will increase Fe^{2+} ion concen tration, which acts as donor, and thus reflecting in n type enhanced conductivity. However, observed increase in activation energy may be attributed to scattering effects. Johnston et al.[27] also have attributed the increase in E value to tetrahedral Ti^{4+} ions, which acts as a scattering centre for hopping of electrons.

Moreover the grain size, density and the micro structure also influence the bulk conductivity of the ferrite materials. Incorporation of Zr^{4+} ions in the lattice of $Zn_xMg_{1-x}Fe_2O_4$ ferrite system brings about following effects in the behaviour of the system and thus influences the bulk electrical conductivity of the material.

1) It probably increases the Fe^{2+} ion concentration giving rise to n type conductivity to the bulk in almost all the ferrite samples.

2) It affects the grain size, density and micro structure (discussed in Chapter II)[26]

3) An increase in the grain size will increase the bulk conductivity, being determined by sintering temperature.

4) An increase in the density increases the bulk conductivity, by suppressing the preferential oxidation states of the grain boundries. Presence of closed pores at grain boundries faciliates oxidation of the grain boundries during cooling after sintering.

5) Zr^{4+} ion entering into the lattice may segregate near the grain boundries thereby increasing its effective thickness and so decreases the bulk electrical conductivity to some extent.

Segregation of titanum^{4+} in Mn-Zn ferrite and vanadium^{5+} in Ni-Zn ferrite, referred above have the strong evidences from Auger Spectroscopy[24,25]

The second region of conductivity in L0, L2, L4, L6 samples can be attributed to phase transition by many workers[7,10]. Nanba[7] et al. have attributed this to cation migration, while Rezlescu et al.[11] to cation ordering. We have attributed this phase transition by cation migration, which shows increased conductivity in this region. This region has been attributed to the change of spin from colinear to a special case of triangular spin by Todkar et al.[10], in fact the Y-K angles are calculated by us and we have observed this sort of change will be presented in the next chapter IV.

The values of characteristic temperature 'Th' are found to depend on composition similar to Curie temperature, that both decreases with increase of zinc content. The experimentalTc values are in good agreement to that of calculated from log (ρ) versus temperature plots. The samples L0, L2, L4, L6 shows second break at 'Tc' the Curie temperature, while L8 shows first break at Tc beyond it all are paramagnetic. The increase in activation energy (ΔE) clearly show this change from ferri to para region. If the concept of Elwell

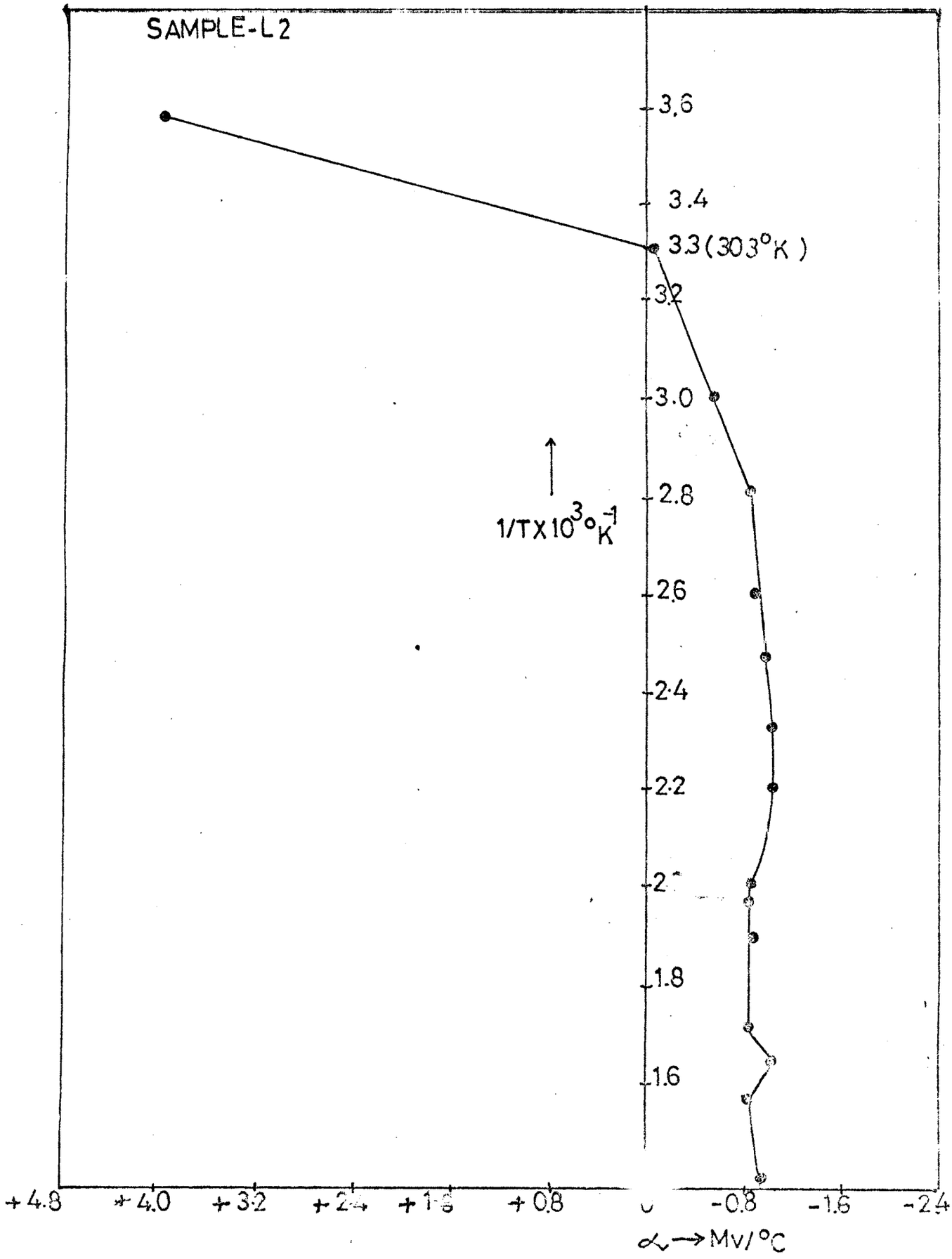

FIG-3.12:- $1/T \times 10^3\,°K^{-1}$ X Seeback coeff α-Mv/°C

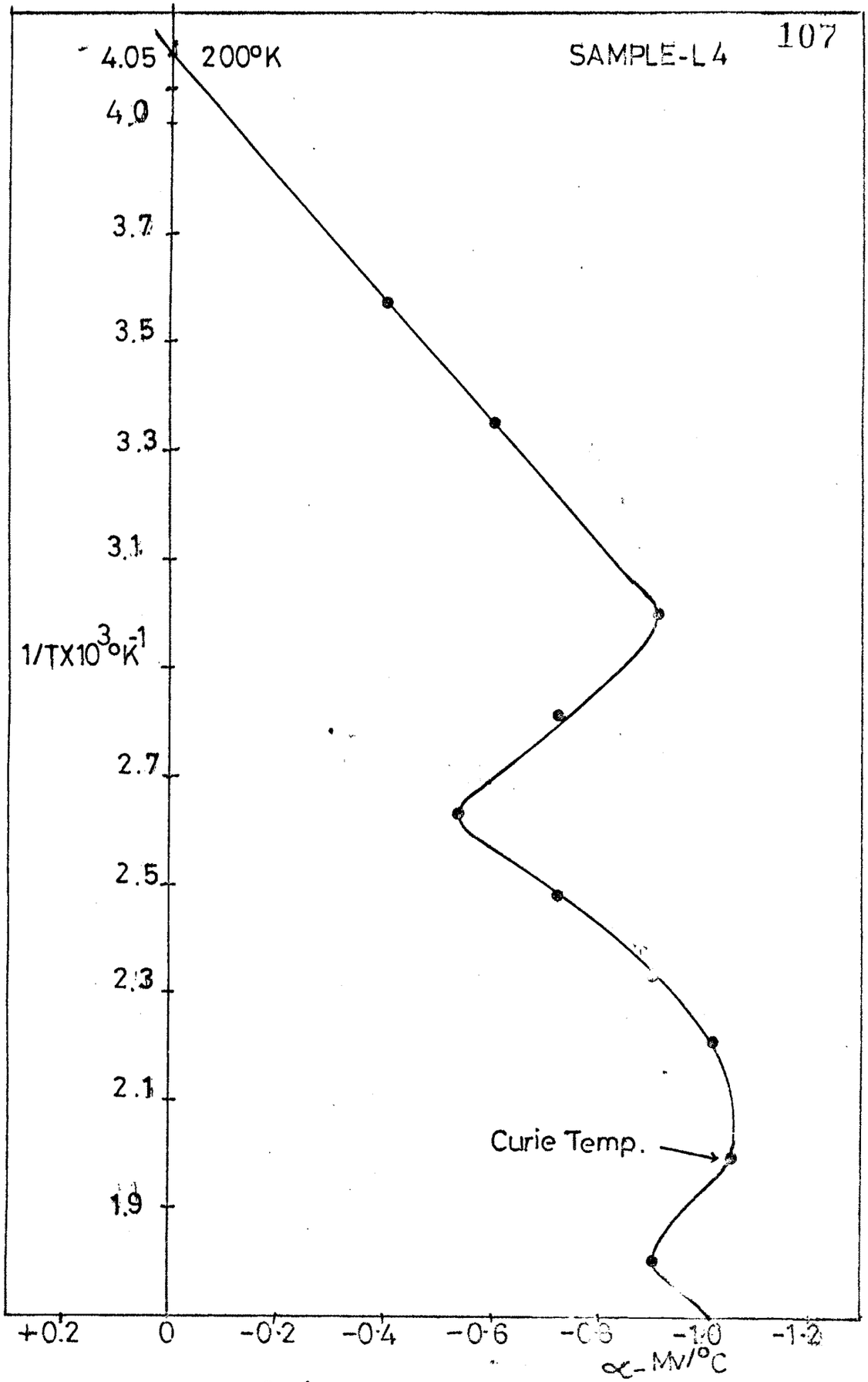

FIG 3.13 : $1/TX10^{3}$°K^{-1} X Seebeck Coeff ∝ -MV/°C

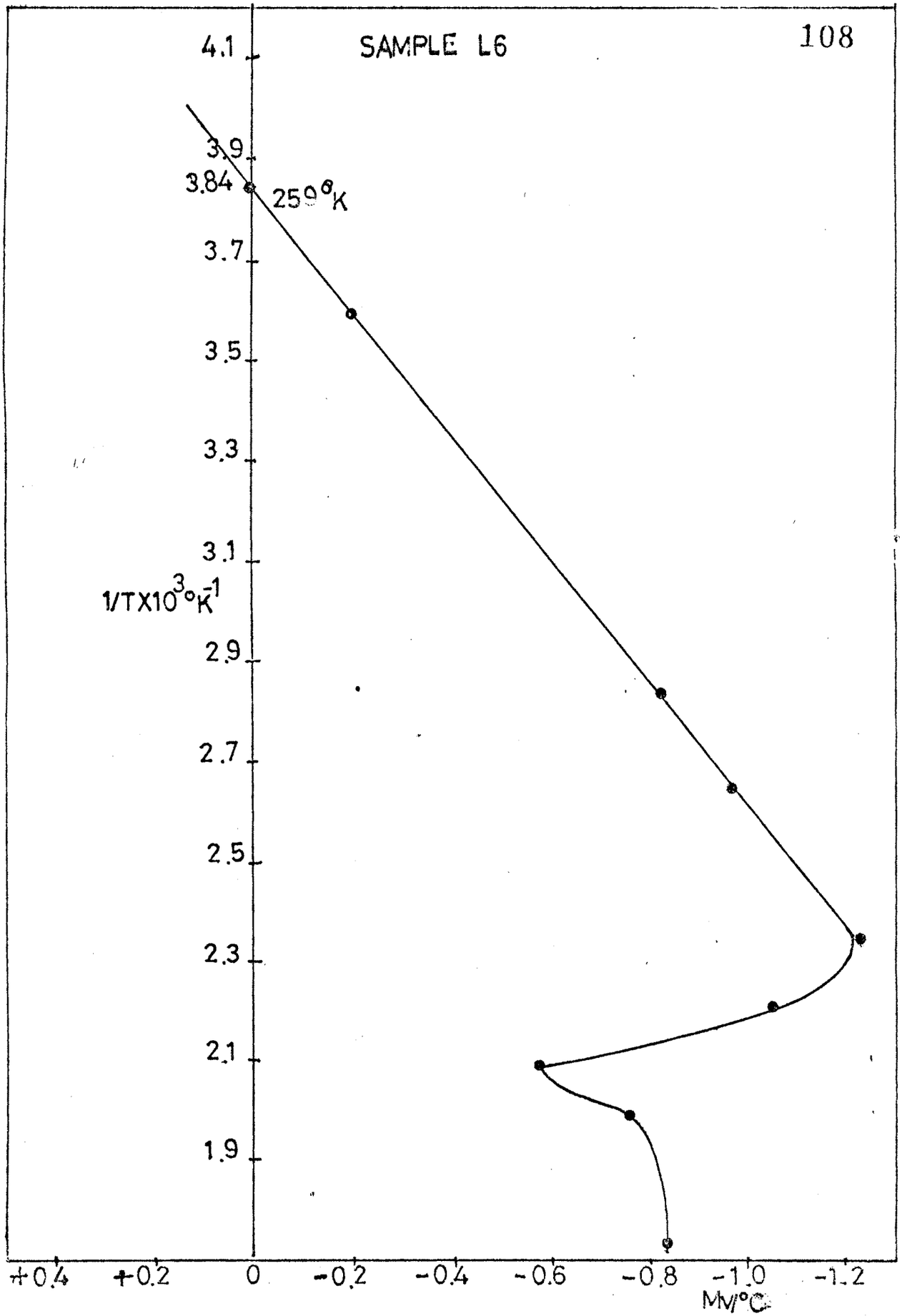

FIG- 3.14 : $1/TX10^{3}{}^{\circ}K^{-1}$ X Seebeck Coeff α – MV/°K

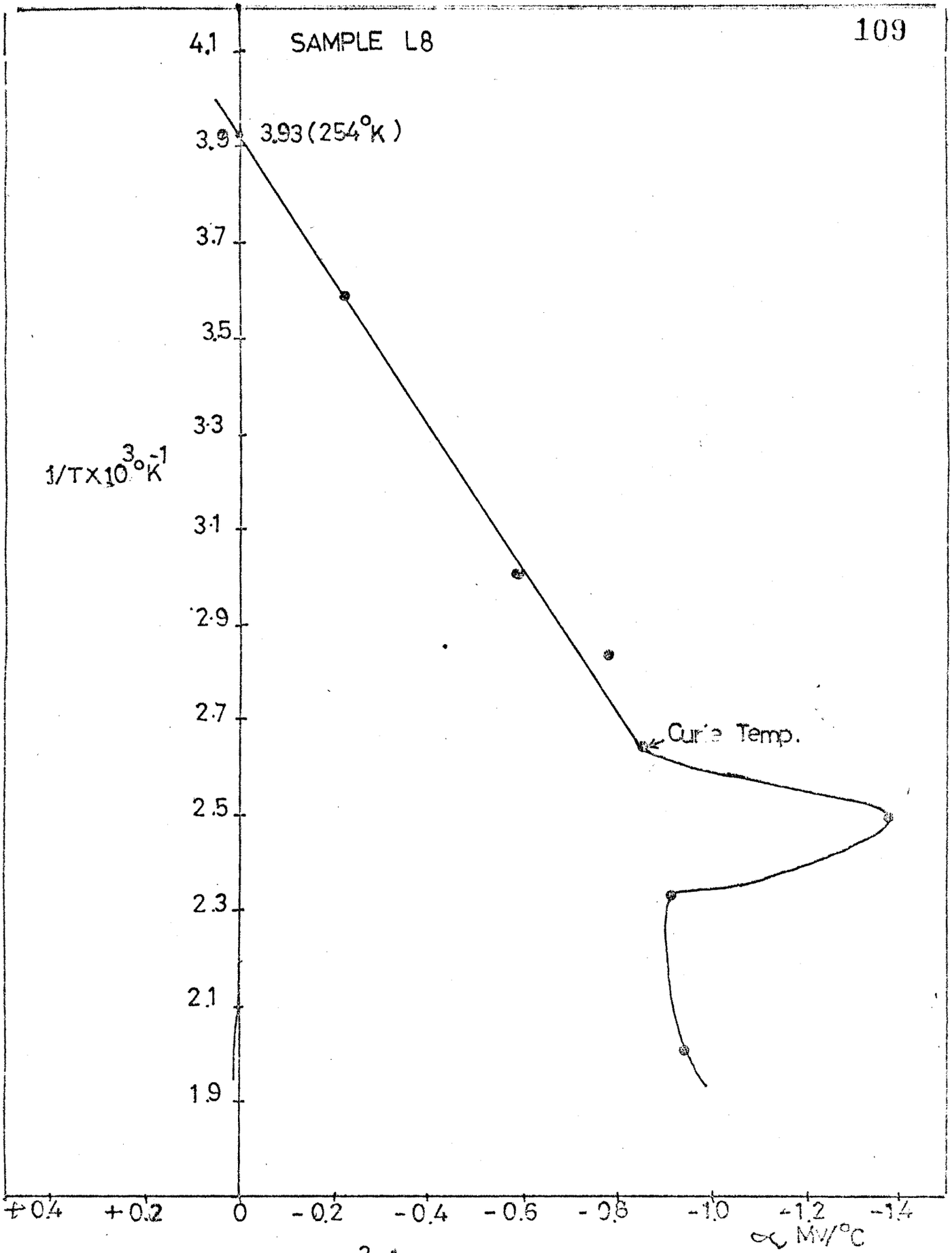

FIG 3.15: 1/T X 10^{3} °K^{-1} ∝ MV/°C

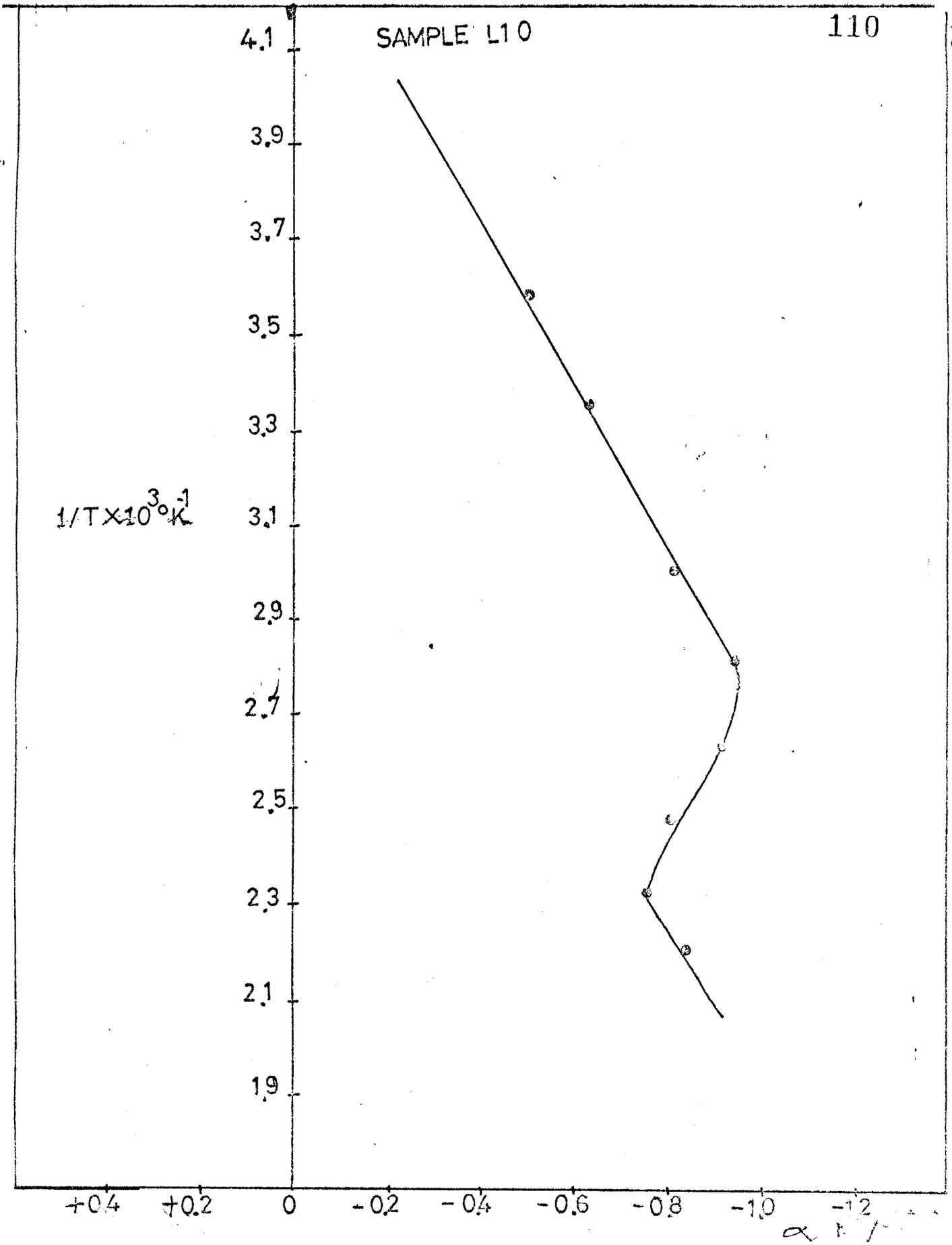

EIG-3.16 : $1/T \times 10^{3\circ}K^{-1}$ X α MV/°C

and Dixon[27] is employed (who has co-related ' E' and 'ω), it can be concluded that in a third region conduction is due to thermally activated polaron hopping process, which is discussed at the beginning of this section, while discussing the general trend of conduction.

The sample L10 i.e. $ZnFe_2O_4$ doped with 0.01% mol.wt.% ZrO_2, show only one regioin of conductivity can be attributed to its paramagnetic nature at and above room temperature. By inspection of figures (3.5 to 3.10) of log (ρ) versus 1/T, it can be observed that with increasing zinc content the three region structure goes on diminishing. It is very predominant in L0 and does not exist in L8, where it shows purely two region structure.

REFERENCES

1) Verway E.J.W., Haayman D.W., Ramejin F.C., Van Oosterhaut G.W., Phillips Res. Rep. 5, 173 (1950).

2) Miyata N., J. Phys. Soc. Japan 16, 206 (1961).

3) Jonkar G.H. and Van Santen S., Physica 19, 120 (1953).

4) Komar A.P. and Kliushin V.V., Bull. Acad. Sci. USSR 18, 403 (1954).

5) Van Uiteret L.G., J. Chem. Phys. 23, 1883 (1955).

6) Klinger M.I., J. Phys. C. (G.B.) 8, No.21, 2595 (1975).

7) Nanba N.J., Appl. Phys. 49, 2950 (1978).

8) Ghani A.A. and Miryasov No.2, Sov.Phys.Solid State (USA) 13, 2627 (1972).

9) Joshi G.K., M.Phil. Thesis, Shivaji University, Chapter III, (1986).

10) Todkar M.M., Ph.D.Thesis, Shivaji University, Chapter III,V (1987).

11) Reziescu N., Rezlescu E., Solid State Comm. 14, 69 (1974).

12) F.C. Brown, I.G.Austen, and N.F.Mott, Advances in Physics 18, 41 (1969).

13) Heikes R.R., Johnston W.D., Jr.Chem. Phys. 26, 582 (1957).

14) Parker R., Phil. Mag. 3, 853 (1966).

15) K.K. Loria, A.P.B.Sinha, Ind. J. Pure and applied Phys., 1, 215 (1963).

16) Komar A.P. and Klivish V.V., Bull. of acad. sciences USSR Phy. 18, 96 (1954).

17) Sisma Z., Zech J. Phys., B 16, 99 (1966).

18) Jonkar G.H., Van Hauten S., Halbieterprobleme 6, 118 (1961).

19) Sawant S.R., Patil R.N., Indian Journal of Pure and applied Phys., 20, 353-355 (1982).

20) N. Rezlescu and E. Cuclureanu, Phy. Stat. Sol. (9) 3, 873 (1970).

21) Ghani A.A., Eatah A.I. and Mohamed A.A., Ferrites, Proc. Int.Conf. Japan Sept.Oct., 216 (1980).

22) Rosenberg M., Nicolau P. and Bunzet I., Phys. Status Solidi. 15, 521 (1966).

23) Standley K.J., Oxide Magnetic Materials, Clearndon Press, Oxford 1972.

24) Ram Narayana, R.B.Tripathi, B.K.Das, G.C. Jain, Jr. of Mater. Sci., 18, 1933-40 (1983).

25) D.W.Johnston, Jr. D.K.Gallagher, M.F. YON and H.Schrieber, J. solid State Chem., 30, 229 (1979).

26) Ram Narayan, R.B.Tripathi and B.K.Das, J. Mater. Sci., 18 (1983) 1267 (Part I of this paper).

27) Elwell D. and Dixon A. Solid State Comm. 6, 585 (1968).